

DETERMINE CHARACTERISTICS REQUIREMENT FOR THE SURROGATE ROAD EDGE OBJECTS FOR ROAD DEPARTURE MITIGATION TESTING

Stanley Chien

Qiang Yi

Jun Lin

Abir Saha

Lin Li

Yaobin Chen

Indiana University-Purdue University Indianapolis

USA

Chi-Chih Chen

Ohio State University

USA

Rini Sherony

Collaborative Safety Research Center, Toyota Motor North America

USA

Paper Number 19-0059

ABSTRACT

Road departure mitigation system (RDMS), a vehicle active safety feature, uses road edge objects to determine potential road departure. In the U.S., 45%, 16%, and 15% of car-mile (traffic flow * miles) roads have grass, metal guardrail, and concrete divider as road edge, respectively. It is difficult to test RDMS with real roadside objects. Lightweight and crashable surrogate roadside objects that have representative radar, LIDAR and camera characteristics of real objects have been developed for testing. This [paper describes the identification of automotive radar, LIDAR, and visual characteristics of metal guardrail, concrete divider, and grass](#). These characteristics will be referenced for designing and fabricating the representative surrogate objects for RDMS testing. Colors and types of the roadside objects were identified from 24,735 randomly sampled locations in the US using Google street view images. The radar and LIDAR parameters were measured using 24GHz/77GHz radar and 350-2500nm IR spectrometer.

Metal guardrail: The peak 24GHz RCS (Radar Cross Section) of W-beam and I-beam of guardrail are 10dB and 13dB. The peak 77GHz RCS for W and I-beam are 15dB and 20dB. When the radar beam direction is not perpendicular to the metal guardrail surface, the reflectivity decreases significantly. As the illumination/measurement angle increases from 0 to 70°, the IR reflectance of metal guardrail decreases from 1.3 to 0.1, and the variation among samples decreases from 1.5 to 0.05. The age of the metal guardrail does not affect the RCS if steel rust is not present.

Concrete divider: Both 24GHz and 77GHz radar reflectivity are -7.3dB. The age of the concrete divider does not affect the radar reflectivity, but the surface smoothness and material affect the reflectivity. As the illumination/measurement angle increases from 0 to 70°, the IR (Infrared) reflectance of concrete divider increases by only 0.1.

Grass: The peak 77GHz RCS is -18dB at 10° depression angle. Different kinds of grass (wild vs. maintained, short vs. long, even vs. uneven) have similar RCS value when measured under the same conditions (same radar type, same polarization, and same pitch angle). Same grass field will produce different RCS during different seasons or after rain where the moisture content of grass produces different reflectivity. As the illumination/measurement angle increases from 0 to 70°, the IR reflectance of grass increases from 0.1 to 1 and the variation among samples increases from 0.2 to 1. The most representative grass road-edge is uneven yellow/green mixed short grass followed by even green and short grass. 18 most occurring grass color patterns were selected.

This is the author's manuscript of the article published in final edited form as:

Chien, S., Qiang, Y., Lin, J., Saha, A., Li, L., Chen, Y. (2019). Determine characteristics requirement for the surrogate road edge objects for road departure mitigation testing. The 26th ESV 2019 – Technology: Enabling a Safer Tomorrow.

INTRODUCTION

According to the U.S Department of Transportation Federal Highway Administration, over half of the fatal vehicle crashes were related to road departure [1]. A vehicle road-departure crash is defined as when the vehicle moves from the road to the roadside and consequently leads to a crash [2, 3]. Road departure warning (RDW) and road keeping assistance (RKA) [4-12] are the new technology for reducing road departure crashes [13, 14]. The road departure detection can be based on the recognition of road edge markings. However, many US roads do not have road edge marking or clear road edge marking. Therefore, road edge detection needs to rely on the detection of roadside objects, such as grass, concrete divider, metal guardrail, etc. As RDW and RKA technologies are based on the detection of a roadside object, their performances need to be tested with the roadside objects. The performance testing of the RDW and RKA cannot be on the road with real roadside objects. Testing the RKA on the road with a real concrete divider or real metal guardrail is quite difficult. Testing the RDA on the road with grass road edge is also difficult. The test track may not have a proper grass road edge for RKA tests. To support the performance testing of RDW and RKA, surrogate roadside objects need to be developed so that the test can be performed on the test track repeatedly. Transportation Active Safety Institute (TASI) of Indiana University–Purdue University Indianapolis (IUPUI) studied the development of surrogate roadside objects for RDW and RKA testing with the support of Toyota Collaborate Safety Research Center (CSRC). This paper summarizes the representative shape, color, radar, LIDAR characteristic of the commonly seen roadside objects, such as concrete divider, metal guardrail, and grass. These characteristics can be used as the characteristics requirements for designing and fabricating the object surrogates. The design and fabrication of object surrogates are not in the scope of this paper and will be described in other papers.

MOST COMMON ROADSIDE OBJECTS

In our previous study [15], we sampled 24,762 Google Street view locations all over the United States. Based on location counts, we found that 55% locations have grass edge, 16% locations have concrete curbs, 8.68% locations have a metal guardrail, and 4.17% locations have the concrete divider as the road boundary. If we consider the traffic density on these locations (based on car-miles), we found that 44.6% locations have grass edge, 9.9% locations have concrete curbs, 16.1% locations have metal guardrails, and 15.3% locations have concrete dividers as the road boundary. Since concrete curb is mostly on the city roads with low-speed limits and RDW and RKA are mainly designed for roads with higher speed limits, metal guardrail, concrete divider, and grass road edges are the most common road edges detected by RDW and RKA. Since camera, 24 GHz and 77GHz radar, and automotive 800-1100 nm LIDAR are the most common sensors used for object detection in vehicle active safety, the scope of this paper is to present the representative characteristics of metal guardrail, concrete divider, and grass in the view of the camera, 24 GHz and 77GHz radar, and automotive 800-1100 nm LIDAR.

SPECIFICATIONS OF SURROGATE METAL GUARDRAIL

Physical Shape of the Representative Metal Guardrail

In aforementioned 24,735 randomly sampled road locations in the US, 2150 locations have various types of metal guardrails on the roadside. 81% of these 2,150 metal guardrails has horizontal W-beam with I-beam support (Fig. 1). The representative shape specifications of W-beam and I-Beam in the US can be found in [16]. The representative RGB color of the metal guardrail is (138,139,139) [17]. The physical shape specification of metal guardrail in other countries may be different.






RGB	Range (10% brightness)	
138, 139, 139	168, 168, 168	112, 113, 112
		

Fig. 1. Representative metal guardrail W-beam (left), and color (right).

Radar Characteristics Specifications of Representative Metal Guardrail

Since the metal guardrail surrogate is composed of the W-beam surrogate and the I-beam surrogate, the 24GHz and 77GHz RCS of five W-beams and I-beams were measured. The objects were placed on a rotating table, and their RCS at various angles were measured. The representative RCS of these objects are plotted in Fig. 2 to Fig. 5. Arrows in these figures and orientation of these objects show the viewing angles of the W-beams (blue) or I-beams (gray). The important RCS values that show the characteristics of the objects with respect to the viewing angles are circled. A variation of $\pm 2\text{dB}$ for each circled value is observed with different samples. It was found that the age of the guardrail has little effect on their RCS values (assume the guardrail is not rusted).

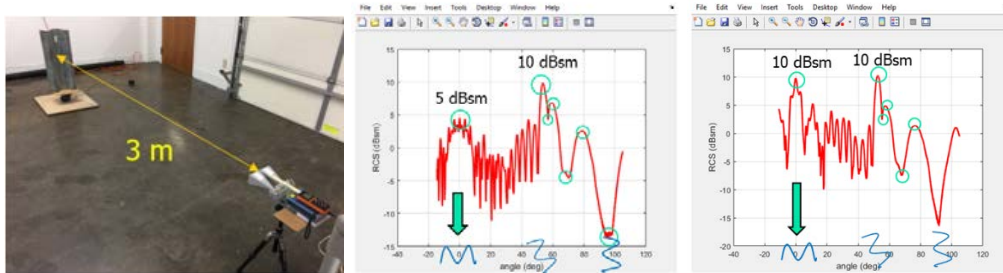


Fig. 2. 24GHz RCS of W-beam. Measurement (left), vertical polarization (middle) horizontal polarization (right).

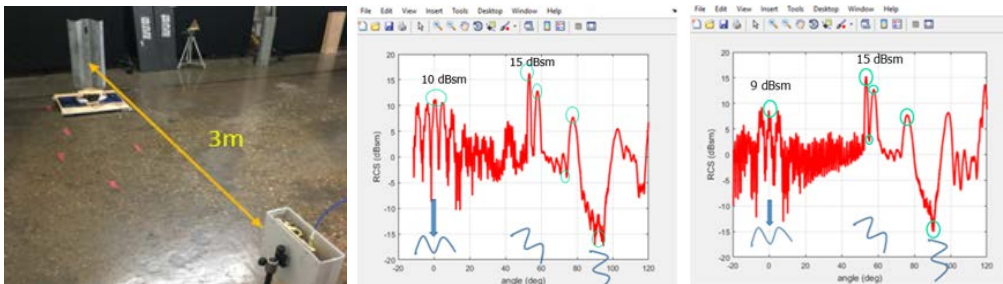


Fig. 3. 77GHz RCS of W-beam. Measurement (left), vertical polarization (middle) horizontal polarization (right).

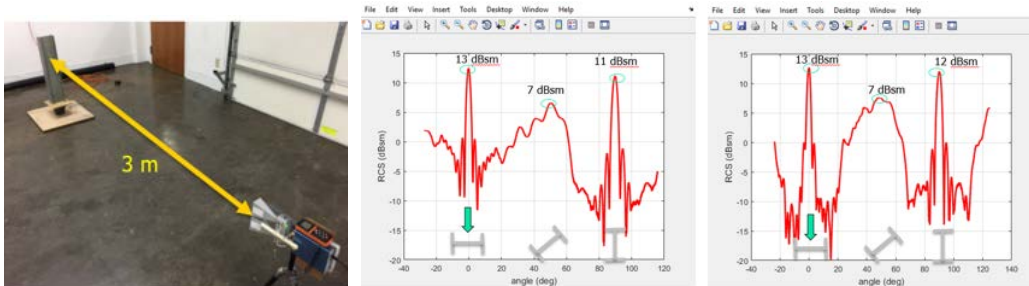


Fig. 4. 24GHz RCS of an I-beam. Measurement (left), vertical polarization (middle), horizontal polarization (right).

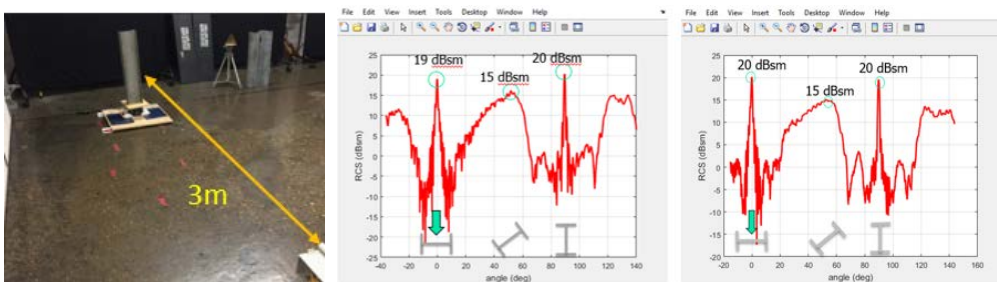


Fig. 5. 77 GHz RCS of an I-beam. Measurement (left), vertical polarization (middle), horizontal polarization (right).

LIDAR Characteristics of Representative Metal Guardrail

There is not a standard laser wavelength for the automotive LIDAR. Common automotive Lidar's wavelengths are in the range of 800-1100nm. We used a spectrometer to measure the diffusive reflectivity of 4 galvanized metal surface samples at various viewing angles. The light source and the measurement probe were put as close as possible to mimic the LIDAR operation. Multiple points on each sample surface were measured. Fig. 6 shows the upper and lower boundaries of the representative IR reflectivity of metal guardrail surface in various laser wavelengths at various measurement angles. 0 degree means that the LIDAR beam is perpendicular to the surface being measured. Since the IR reflectivity variation is small and we do not have a large sample set, the upper bound is the measured maximum reflectivity value plus 0.02, and the lower bound is the measured minimum reflectivity value minus 0.02. It can be seen that the IR reflectivity of the metal guardrail decreases as the viewing angle is getting away from the perpendicular direction to the measured surface. The diffusion reflectivity is only applicable for diffusion surface and should be less than 1 in concept. However, the metal guardrail shows the specular reflection property when measured in low angles (0 to 15 degrees) and shows the diffusion reflection property when measuring in high angles (20 degrees and up).

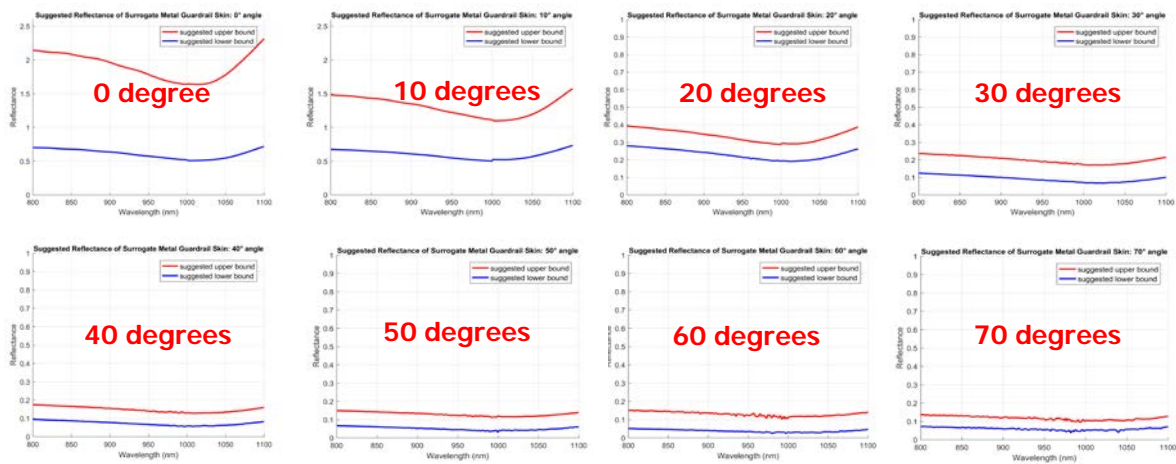


Fig. 6. Suggested IR reflectance range of metal guardrail surface from various viewing angles.

SPECIFICATIONS OF CONCRETE DIVIDER AND CURB SURROGATES

Physical Shape of the Representative Divider and Curb

Concrete curb has many different shapes. In aforementioned 24,735 randomly sampled road locations obtained from Google Street View images, 66% of the 856 concrete dividers observed are in F shape, New Jersey, and single slop shapes. We selected F-shape as the representative shape of the concrete divider. The representative shape specifications of F-shape concrete divider and curb in the US are shown in Fig. 7 [15]. The representative RGB color of concrete divider and curb in the US is (168, 161, 149) [17]. The representative shape and color of the concrete divider in other countries may be different.



Fig. 7. Standard dimensions F-shaped concrete divider (left) curb (right).

Radar Characteristics of Representative Concrete Divider and Curb

Since the concrete divider has a large flat surface, its radar characteristics cannot be described by RCS. Therefore, we use the radar reflectivity to describe the radar property of the concrete divider surface. The proper surface reflectivity property and the correct shape of the surrogate will make it have the correct radar property of a real concrete divider. According to the 24GHz and 77GHz radar reflectivity measurements, forward-looking radar cannot detect concrete divider from a depression angle greater than 15 degrees. So all reflectivity measurement is measured with the radar beam perpendicular to the concrete surface. The measurement results of 7 concrete dividers and curbs suggested that both the representative 24GHz and 77GHz radar reflectivity of common smooth concrete divider surface are -7.3 ± 1 dB under dry condition. The average reflectivity of concrete dividers with smooth surfaces are similar. As the surface is damaged with scratches, the reflectivity varies significantly. The radar reflectivity of the concrete surface increases with the increase in humidity. The color, protective coating, and age of the concrete dividers do not affect their radar reflectivity.

LIDAR Characteristics of Representative Metal Guardrail

A spectrometer that covers a large range of laser wavelength was used to measure the diffusive reflectivity of 7 concrete dividers and curbs of various ages at a range of viewing angles. The light source and the measurement probe were put as close as possible to mimic the LIDAR operation. Multiple points in each sample were measured. Fig. 8 shows the upper and lower boundaries of all measurements at various angles, where 0 degree means that the LIDAR beam is perpendicular to the surface being measured. The upper bound is the measured maximum reflectivity value plus 0.05, and the lower bound is the measured minimum reflectivity value minus 0.05. It can be seen that the IR reflectivity of the concrete surface increases as the viewing angle is getting further away from the perpendicular direction to the concrete surface. The concrete surface is diffusive in all viewing angles.

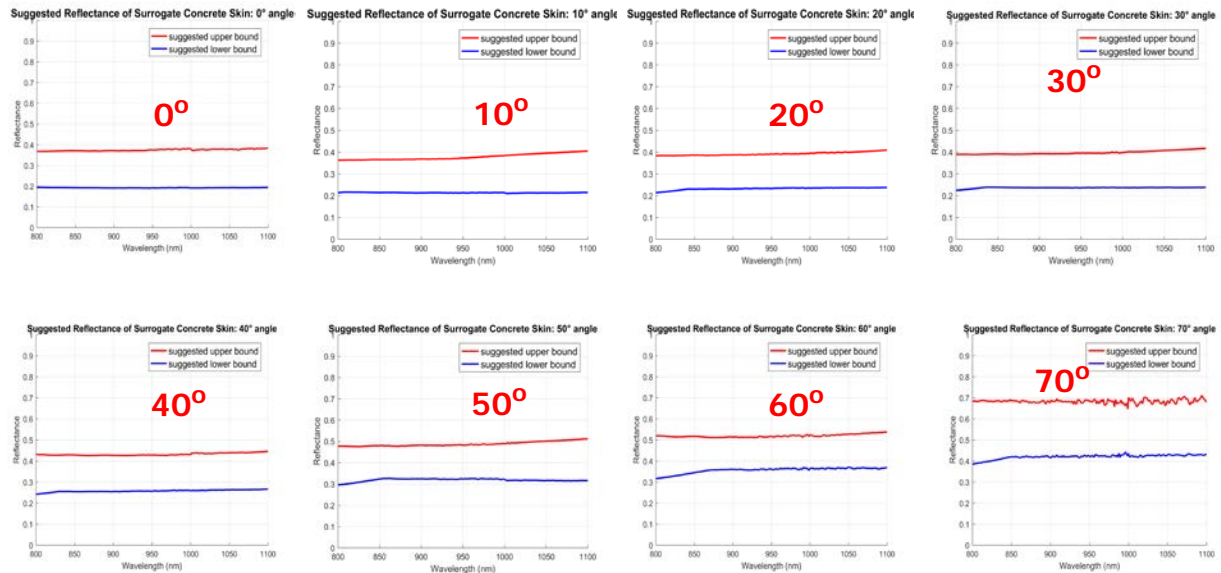


Fig. 8. Representative IR reflectance range of concrete surface from various viewing angles.

SPECIFICATIONS OF GRASS SURROGATES

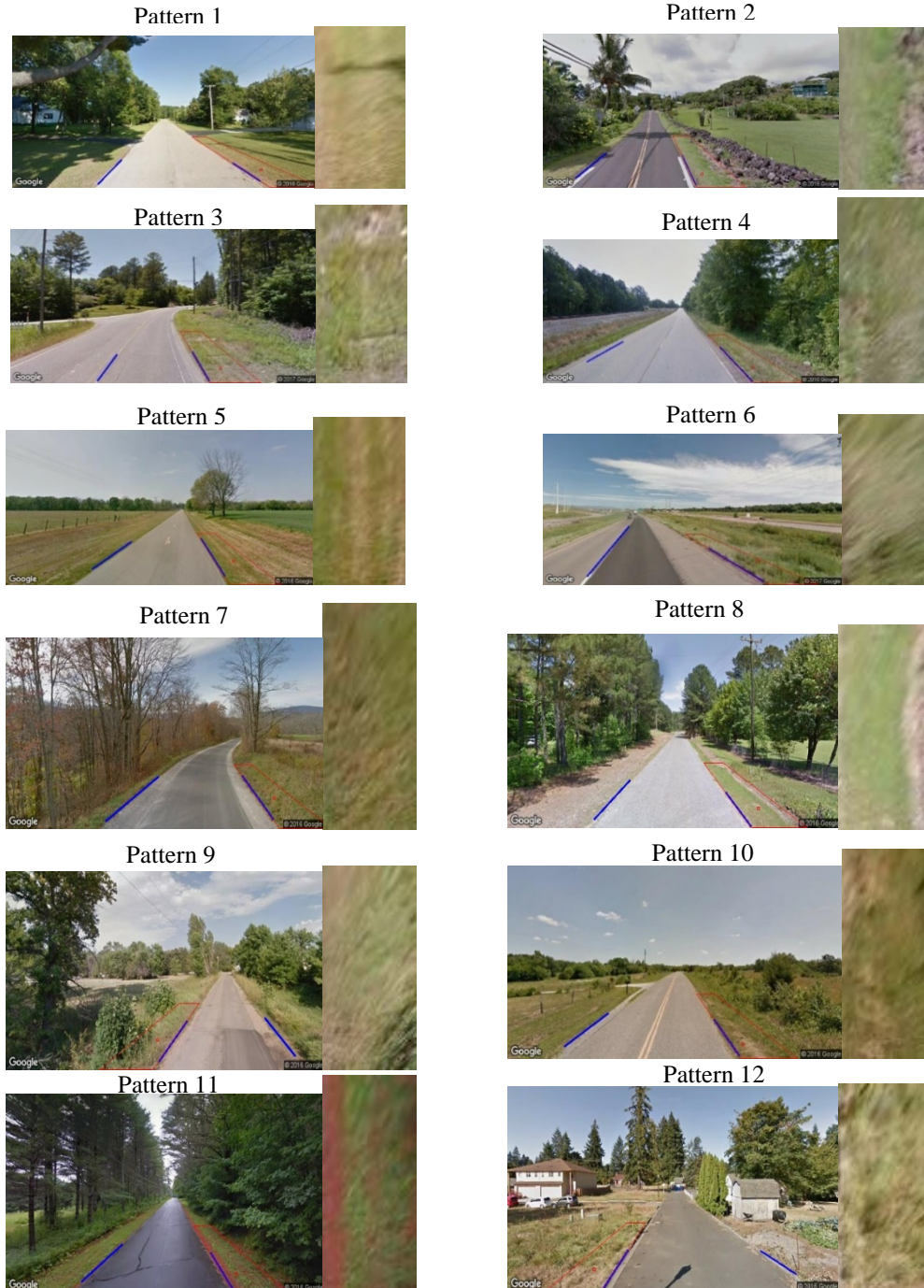
Height and Color of Representative Grass

In the aforementioned 24,762 Google Street View images, the RGB color of 901 grass images in good weather and not under the shade were studied. The heights of grass in the images were estimated based on over 70 reference road images with known grass height of the grass road edge. The conclusion was that the height of over 80% roadside grass was short (2-4”) or medium (5-10”), about 46% of the roadside grass were mixed green and yellow, about 30% grass was green, and rest was brown/yellow. The color of the grass samples was clustered into 6 groups with the representative color as shown in Table 1. Since the grass color patterns have vast variations, we clustered the 901 grass samples and generated 18 color patterns (see

Fig. 9). For each color pattern, the left is an example image, and the right is the actual color pattern. Each color pattern can be a mix of several colors identified in Table 1.

Table 1.
Representative color components of grass.

Color	Yellow			Green		
R,G,B	111, 95, 65	146, 130, 96	170, 162, 135	99, 100, 55	105, 110, 44	139, 141, 87



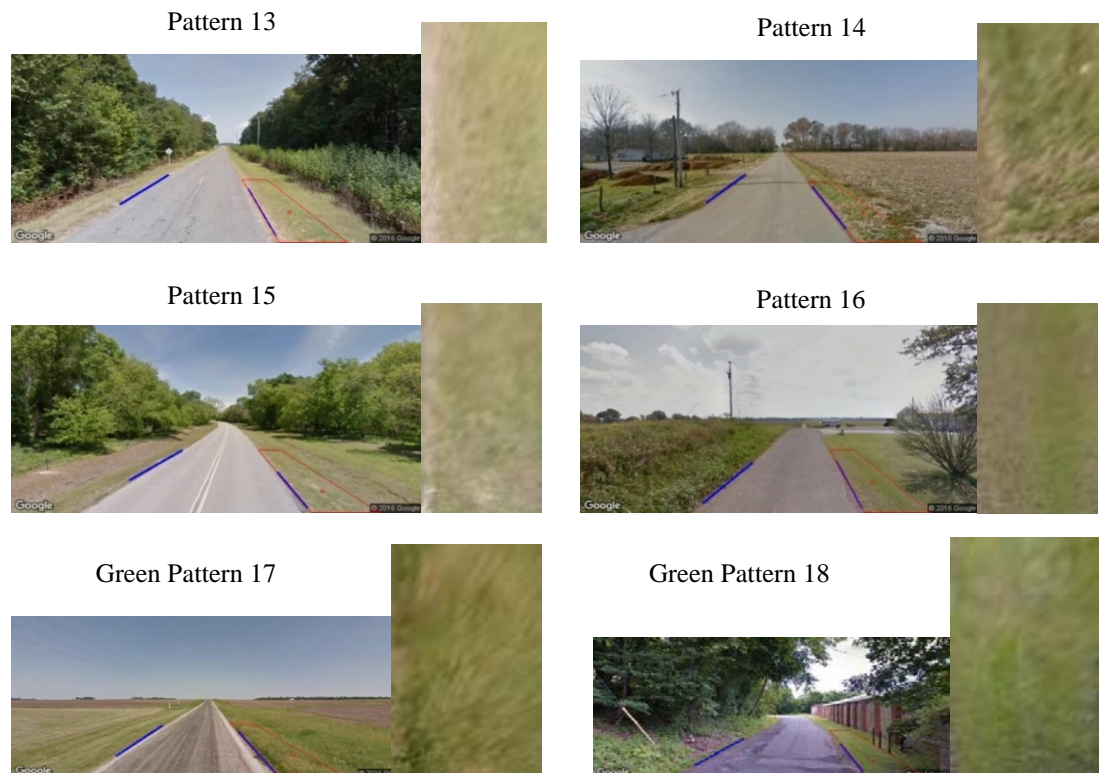


Fig. 9. Grass color patterns.

Radar Characteristics of Representative Grass

24GHz RCS and 77GHz RCS were measured on three grass samples. The physical appearance of these grass samples is shown in Table 2. The radar set up is illustrated in Fig. 10. The maximum, minimum, average and mean 77GHz RCS measurement result of these grass samples are in Fig. 11. The maximum, minimum, average and mean 24GHz RCS measurement result of these grass samples are in Fig. 12. The x-axis of the plot is the distance of the grass to the radar. The Y-axis is the RCS value. The blue vertical line indicates the location of the reference corner reflector. The RCS on the left of the vertical blue line is heavily influenced by antenna coupling and is not useful. The RCS on the right side of the dashed box is too weak and can be considered as background noise. The slope of the RCS plot in the region covered by the dashed box illustrates the RCS characteristics of the grass.

Table 2.
Grass samples used to measure 77GHz RCS.

Grass	Height	Color	Surface Condition	Type
1	Short (2-4 inches)	Green and Yellow	Somewhat even	Wild
2	Medium (8-10 inches)	Green and Yellow	Uneven	Wild
3	Short (2-4 inches)	Green	Very even	Well maintained

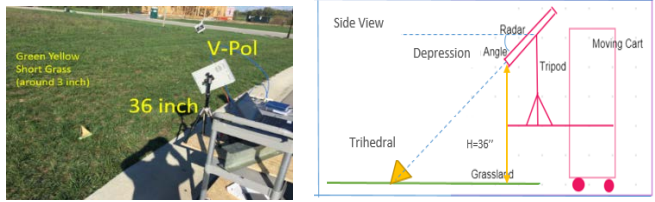


Fig. 10. Grass 77GHz RCS measurement.

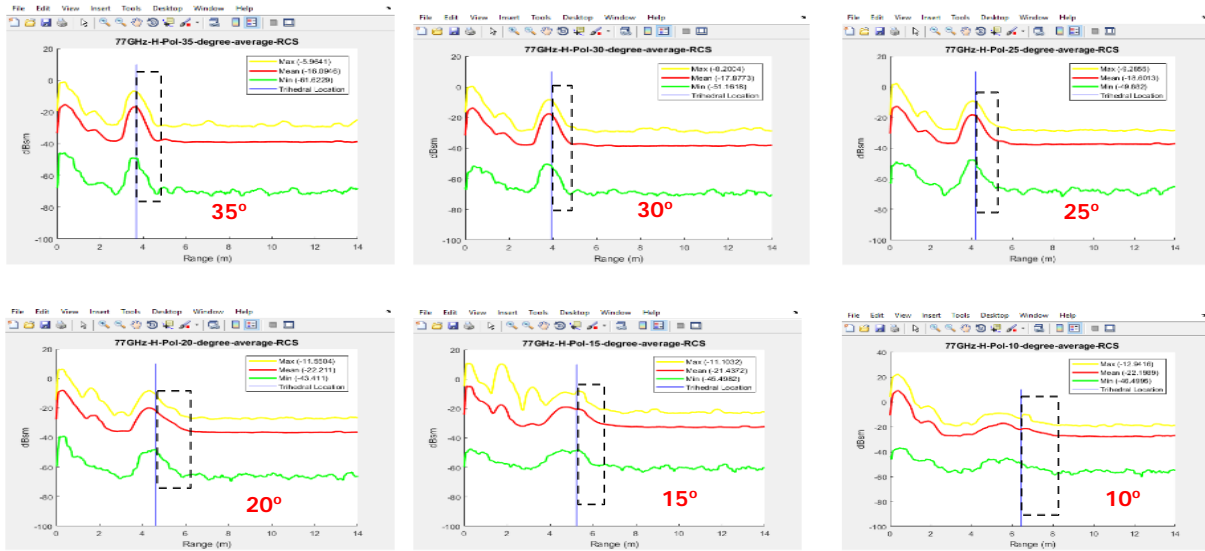


Fig. 11. Grass RCS Recommendation (77GHz Horizontal Polarization).

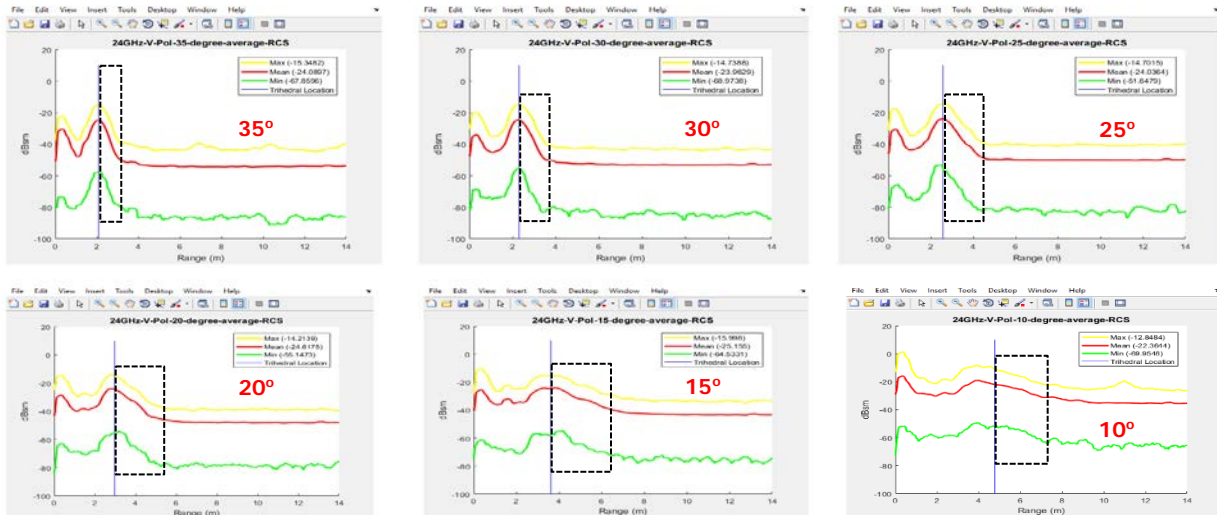


Fig. 12. Grass RCS Recommendation (24GHz Horizontal Polarization).

LIDAR Characteristics of Representative Grass

A spectrometer that covers a large range of light wavelengths was used to measure the diffusive reflectivity of 6 grass samples in indoor and outdoor at a range of viewing angles. The light source and the

measurement probe were placed as close as possible and aimed in the same direction to mimic the LIDAR operation. Multiple points were measured on each sample. Fig. 13 shows the upper and lower boundaries of all measurements at various angles, where 0 degree means that the LIDAR beam is perpendicular to the surface being measured. The upper bound is the measured maximum IR reflectivity value plus 0.05 and the lower bound is the measured minimum IR reflectivity value minus 0.05. It can be seen that the IR reflectivity of the grass increases as the viewing angle is getting further away from the perpendicular direction. The grass starts to show specular reflectivity when the measurement angle is above 50 degrees. The IR reflectivity also increases as the infrared wavelength increases in the 800-1100nm range.

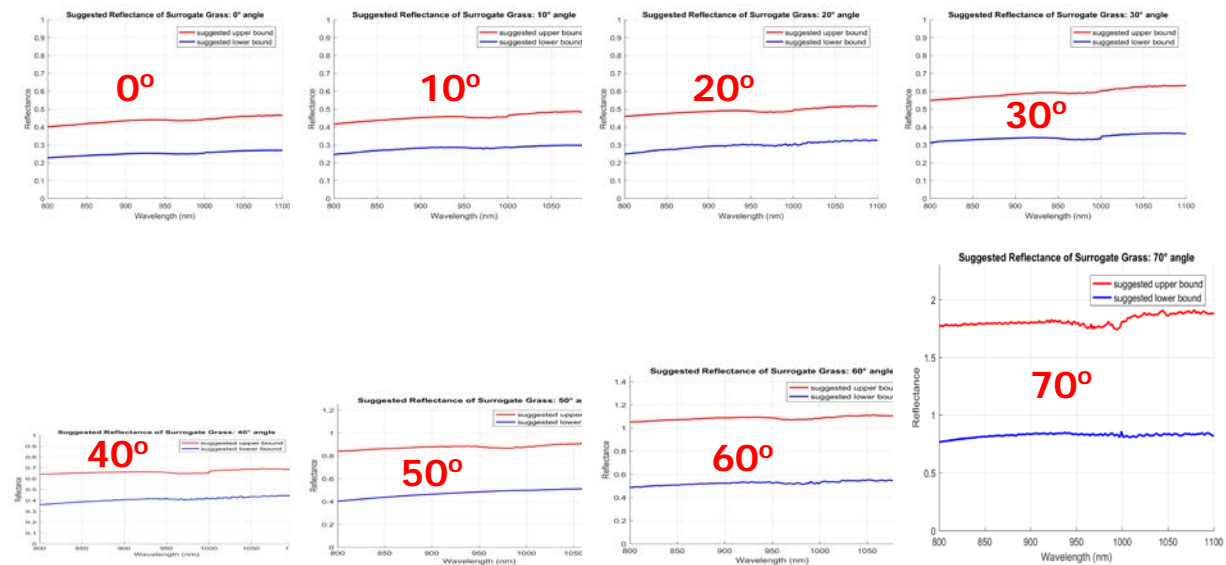


Fig. 13. The IR reflectance of grass fields at various measurement angles.

CONCLUSIONS

This paper summarized the 77GHz and 24GHz radar, LIDAR, and camera characteristics of grass, metal guardrail, and concrete divider. This information can be used for the development of grass, concrete divider, and the metal guardrail surrogates, which is essential for the standard evaluation of the Road Departure Warning and Road Keep Assistant systems. Based on this information, we have already developed surrogate grass, guardrail and concrete divider for testing. The design and testing of the surrogates will be described in future publications.

ACKNOWLEDGMENT

This research was sponsored by the Toyota Collaborative Safety Research Center.

REFERENCES

- [1] "Roadway Departure Safety," U.S. Department of Transportation Federal Highway Administration. https://safety.fhwa.dot.gov/roadway_dept/.
- [2] Arora, Prashant, David Corbin, and Sean N. Brennan. "Variable-sensitivity road departure warning system based on static, mapped, near-road threats." In Intelligent Vehicles Symposium (IV), 2016 IEEE, pp. 1217-1223. IEEE, 2016.
- [3] Lattke, Benedikt, Alfred Eckert, Harald Feifel, Dominik Fröhlich, J. Mccaiain, Ganesh Adireddy, Florian Janda, and Erich Fuchs. "Road departure protection-a means for increasing driving safety beyond road limits." In 24th International Technical Conference on the Enhanced Safety of Vehicles (ESV), no. 15-0212. 2015.
- [4] Harry W. Taylor, "Preventing Roadway Departures," US Department of Transportation Federal Highway Administration. <https://www.fhwa.dot.gov/publications/publicroads/05jul/03.cfm>.

- [5] Charles F. McDevitt, "Basics of Concrete Barriers," *Public Roads Magazine*, <https://www.fhwa.dot.gov/publications/publicroads/00marapr/concrete.cfm>.
- [6] Sparbert, Jan, Klaus Dietmayer, and Daniel Streller. "Lane detection and street type classification using laser range images." In *Intelligent Transportation Systems, 2001. Proceedings. 2001 IEEE*, pp. 454-459. IEEE, 2001.
- [7] Kirchner, Alexander, and Th Heinrich. "Model-based detection of road boundaries with a laser scanner." (1998).
- [8] Cramer, Heiko, and Gerd Wanielik. "Road border detection and tracking in non-cooperative areas with a laser radar system." In *Proceedings of German Radar Symposium*, pp. 24-29. Bonn, Germany, 2002.
- [9] Fardi, Basel, Ullrich Scheunert, Heiko Cramer, and Gerd Wanielik. "Multi-modal detection and parameter-based tracking of road borders with a laser scanner." In *Intelligent Vehicles Symposium, 2003. Proceedings. IEEE*, pp. 95-99. IEEE, 2003.
- [10] Lakshmanan, Sridhar, and David Grimmer. "A deformable template approach to detecting straight edges in radar images." *IEEE Transactions on Pattern Analysis and Machine Intelligence* 18, no. 4 (1996): 438-443.
- [11] Kaliyaperumal, Kesav, Sridhar Lakshmanan, and Karl Kluge. "An algorithm for detecting roads and obstacles in radar images." *IEEE Transactions on Vehicular Technology* 50, no. 1 (2001): 170-182.
- [12] Ma, Bing, Sridhar Lakshmanan, and Alfred O. Hero. "Simultaneous detection of lane and pavement boundaries using model-based multisensor fusion." *IEEE Transactions on Intelligent Transportation Systems* 1, no. 3 (2000): 135-147.
- [13] Katzourakis, Diomidis I., Joost CF de Winter, Mohsen Alirezaei, Matteo Corno, and Reinder Happee, "Road-departure prevention in an emergency obstacle avoidance situation." *IEEE Transactions on Systems, Man, and Cybernetics: systems* 44, no. 5 (2014): 621-629.
- [14] Gupta, Rakesh, Ananth Ranganathan, and Jongwoo Lim, "Road departure warning system," U.S. Patent 9,077,958, issued July 7, 2015.
- [15] Dan Shen, Jun Lin, Stanley Chien, Qiang Yi, Renran Tian, Rini Sherony, "Important Roadside Features for the Development of Vehicle Road Keeping Assistance System," 2018 SAE World Congress, Detroit Michigan, April 2018.
- [16] FLH Standard Drawings, <https://flh.fhwa.dot.gov/resources/standard/Std617-11.pdf>,
- [17] Qiang Yi, Dan Shen, Jun Lin, Stanley Chien, Rini Sherony, "The color specification of surrogate roadside objects for the performance evaluation of roadway departure mitigation systems," 2018 SAE World Congress, Detroit Michigan, April 2018.